THEORY OF NANOTUBE NANODEVICES

SLAVA V. ROTKIN
Beckman Institute, UIUC, 405 N.Mathews, Urbana, IL 61801, USA

Abstract. The paper reviews quantum and classical effects which arise in physics of nanotube devices. Knowledge of nanotube electronic structure has been used for a calculation of quantum capacitance and quantum terms in van der Waals energy. Combining analytical theory and quantum mechanical micromodels I worked out a description for nanoelectromechanical devices, for example, electromechanical switch. The theory takes into account van der Waals forces which show up at the nanoscale and result in appearing of a principal limitation for scaling down NEMS structures. A model, which has been derived for a nanotube device electrostatics, includes an atomistic polarizability of the nanotube in a selfconsistent way. This calculation yields a charge density distribution for given external fields and specific device parameters. On the basis of these main elements of continual compact modeling: quantum mechanical description of the nanotube electronic structure, theory of the van der Waals forces, quantum capacitance and continuum mechanics,– a general theory of nanodevices is proposed.

Key words: nanotube, theory, nanodevice, NEMS, MEMS, van der Waals, quantum mechanics, electronic structure, quantum capacitance

1. Introduction

Applied physics of carbon nanotubes is an emerging new area of nanoscience and nanotechnology. Applied physics modeling and device theory at the nanoscale require special techniques that are in between what have been used in solid state physics and methods applicable to molecular systems (Aluru et.al., 2002). I will identify in this paper several approaches that are known to work for devices on the base of carbon nanotubes.

Various carbon, nitride and chalcogenide nanotubes (NTs) have been demonstrated recently (Tenne, 2001; Dai, 2002). A success of synthetic technology immediately resulted in a number of applications. A few to name are: ultrasharp and wear resistant tips for Scanning Probe Microscopy (SPM), Atomic Force Microscopy (AFM) and Scanning Tunneling Microscopy (STM); electron guns for FPD technology and other electron emitters; chemical sensors and gas storage; modified NT–AFM tips which

* Y.G. Gogotsi and I.V. Uvarova (eds.), // Nanostructured Materials and Coatings for Biomedical and Sensor Applications, 257–277.//

are chemically or bio–sensitive; nanotube electromechanical systems, nanotweezers and nanoswitches and, last but not least, nanotube nanoelectronics. I do not pretend to cover here all aspects of device physics of nanotubes or even any substantial part of it. Instead, I will focus on fundamentals of theory of nanodevices and will discuss how the classical description should match the quantum one. Several theoretical methods will be illuminated. Only analytical results will be presented for the sake of clarity. For specific technical characteristics of concrete devices I will refer a reader to original papers.

Graphite-like Systems and Materials, such as nanotubes, fullerenes, onions, Graphite Polyhedral Crystals, nanographites, and many organic macromolecules, are well known to have valence band system generated by pi and sigma valence electrons (Dresselhaus, 1996). The latter ones are localized and, normally, contribute only to mechanical properties of the graphitic material. In contrast, pi electrons are mobile, highly polarizable and define transport, electrical and electromechanical properties.

Many of graphites exhibit similar behavior at the nanoscale: the tendency for nanoscrolling. In the paper (Rotkin, 2002a) we predicted theoretically and demonstrated experimentally formation of scrolls of carbon sp^2–lattices with a characteristic dimension about several nanometers. This scroll size is typical for single–wall nanotubes (SWNTs) and fullerenes, as well as for nanoarches at the edge of natural three–dimensional (3D) graphite. This size was obtained within a Continuum Energetics theory which includes continuum elasticity, microscopic model of van der Waals interactions and surface energy theory (Rotkin, 2001).

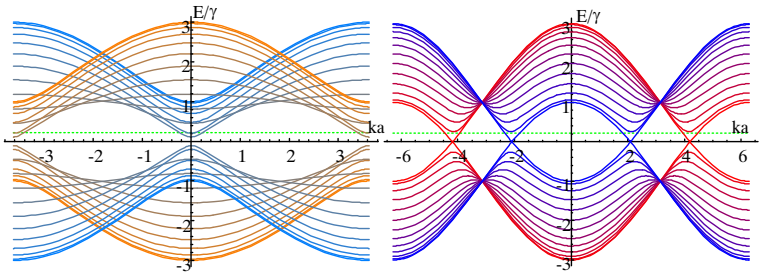

Figure 1. Bandstructure of an armchair SWNT [10,10] (Right) and a zigzag SWNT [17,0] (Left) within first Brillouin zone. Energy is in units of $\gamma \simeq 2.5$ eV, hopping integral.

While the sigma electrons form similar bond lattice in all graphite like (sp^2) substances, which reflects in a close similarity in their morphology as discussed above, a versatility of their electronic properties is due to sensitive electronic structure generated by pi electrons. The electronic structure of a monolayer of graphite (graphene) has a few (six)

Fermi-points where an empty conduction band merges with an occupied valence band. The graphene is a semi–metal (in planar morphology). The pure fullerenes are mainly insulators (perfect spherical morphology). Carbon onions, nanohorns and other imperfect clusters are mainly conducting. The nanotubes may be either metals, or semi–metals (narrow gap semiconductors), or insulators (wide gap semiconductors).

How does an electronic spectrum of a folded SWNT relate to the spectrum of a bare planar graphene? A simple but correct picture of the SWNT bandstructure follows from a band folding argument: we imply extra quantization for one of components of 2D wavevector of the electron in the layer of graphene. This additional space quantization for the pi electrons appears due to confinement in circumferential direction of the SWNT. As a result, 2D surface of the electron energy as a function of 2D wavevector is broken into a number of 1D curves: the nanotube electron subbands. The band folding can be thought of as a mere cross sectioning of the bandstructure of graphene along the nanotube symmetry direction (Fig.1). Depending on the symmetry of the tube, three different situations can be realized: (A) the armchair SWNT has a cross section passing through the Fermi-point. In this case the SWNT is metallic and the conduction band merges with the valence band. (B) The zigzag/chiral nanotube cross section is distant from the Fermi-point. This tube has a nonzero gap and it is a semiconductor tube. (C) One-third of zigzag and chiral nanotubes have a very small gap, which follows from arguments other[1] than simple band-folding. In our simplified picture these SWNTs have a zero band gap and are semi–metals.

The bandstructure of the SWNT is highly sensitive to external fields. Lattice distortions may cause changes in the bandstructure as well. A proper lattice distortion moves the Fermi- point of graphite and results in closing/opening of an energy gap, changing the electron density, and charging the tube. Same is true for an external transverse electric field or magnetic field. An impurity sitting on the nanotube or even placed closely at a substrate surface may have similar action. These phenomena open many possibilities for engineering of NT electronic bandstructure and for application of nanotubes as nano-biosensors, mesoscopic devices and nano-electromechanical systems.

[1] Which is mixing of sigma and pi electrons at a finite curvature. This phenomenon is more pronounced for small radius NT, $R < 4$Å.

2. Modeling of Nanoscale Electromechanical Systems

Nano-electromechanical systems (NEMS) become an essential part of modern science and technology (Craighead, 2000). A number of applications is already known: nanomanipulation, nanosensors, medical devices, nanofluidic devices, to name a few. Even more applications are anticipated as a result of the technological progress in this field.

I address in this section one of issues arising when one tries to understand phenomena happened at the nanoscale with theoretical tools borrowed from macroscopic physics. The latter has to reach its limits and new micromodels are required for a quantitative description of a nano–device. The object of study is a nano–electromechanical switch. Important changes in its operation at the nanoscale are due to van der Waals forces. These forces will change parameters, describing the equation of state of a NEMS. All derivation will be performed analytically, which allows one to apply this theory to a broad class of devices.

2.1. ANALYTICAL MODEL

I start here with a calculation of pull–in[2] parameters of a general NEM system which is an elastic media (elastic manifold) subjected to external forces. The forces are changing during the NEMS operation and define a dynamic shape of the NEMS. The specific forces, considered below, are (i) the van der Waals force, (ii) the electrostatic force, and (iii) the elastic force, which is able to restore the initial equilibrium shape of the NEMS.

In an earlier paper (Dequesnes, 2002a) an analytical derivation as well as a numerical computation of the pull–in voltage, V_o, have been presented with account for the vdW correction. The other pull–in parameter, the pull-in gap, x_o, was treated as an independent quantity and taken from a solution of a classical MEMS problem. Below I will extend the result of the paper (Dequesnes, 2002a) and give an accurate derivation for both pull–in parameters.

The equilibrium dynamic shape of the NEMS satisfies the force balance condition (A): the first derivative of the total NEMS energy is equal to zero. In general, one has to calculate the energy gradient at every point of the manifold and equate it to zero locally. This yields the equilibrium shape of the system at given external forces applied to the NEMS. Main approximation, which allows one to obtain an analytical solution of the problem, is to

[2] The pull–in is a phenomenon of loosing of NEMS stability at a certain (pull–in) voltage. Then infinitely small increase of the voltage results in a sudden collapse of a movable part of NEMS onto a ground plane.

consider only one mechanical degree of freedom[3]. This approximation gives an answer for the pull–in, which is correct up to a geometry dependent numerical factor. The numerical factor is not altered by changing force fields (e.g., by changing van der Waals to Casimir force) and has to be calculated only once for a given geometry or used as a fitting parameter.

Within this one parameter model, I write the first equation of state as: $\frac{\partial E}{\partial x} = 0$ where x is the single degree of freedom of a NEMS, for example, the gap between the elastic movable part of the NEMS and the surface of the ground plane, and E is the total energy given by $E(x,\varphi) = T(x,h;k) - V(x,\varphi;C) - W(x;\epsilon,\alpha)$. Here, the energy depends on x and φ, the gap and the voltage, which are the parameters governing the instability point. Three energy components are the elastic strain energy, T, the electrostatic energy, V, and the van der Waals energy (vdWE), W. All three terms depend on the system geometry, shape, etc., as well as on material parameters (elasticity, capacitance, etc.). The first type of dependence is expressed in terms of the dynamic gap, $0 \le x \le h$; in terms of the maximum separation between the mobile and stationary parts of the NEMS (initial gap), h; and the voltage, φ. The material properties are collected in four constants: an elastic stiffness with respect to the gap, k, a general capacitance with respect to the voltage, C, and general vdW coefficients, α and ϵ. The elastic energy component reads as $T = k(h-x)^2/2$. The electrostatic energy term is $V = C\varphi^2/2$, where the capacitance has to be calculated with a specific micromodel, for example, the model proposed in Ref.(Bulashevich, 2002).

The vdWE energy component is often approximated by a single attraction term (Dequesnes, 2002a; Barash, 1988), which depends on a distance between interacting surfaces. Integrating out all system geometry (Barash, 1988; Girifalco, 2000), one obtains a simple dependence of the vdWE on the gap: $W \simeq \epsilon x^{-\alpha}$, where an exponent α defines the specific power law for the specific dispersion force. For example, for the pure van der Waals interaction between small objects (atoms) $\alpha = 6$, for the retarded Casimir force between atoms $\alpha = 7$, it can be fractional for the many–body terms in low dimensional systems (Rotkin, 2002b; Barash, 1988). With these definitions for the material constants I write the total energy of the NEMS as:

$$E(x,\varphi) = \frac{k(h-x)^2}{2} - \frac{C(x)\varphi^2}{2} - W(x;\epsilon,\alpha) \qquad (1)$$

where the dependence of the capacitance on the gap, $C = C(x)$, has to be defined separately.

To find an instability point of the NEMS I write the second pull–in condition (B): the second derivative of the expression (1) must equal zero.

[3] Which may be thought as a fundamental mechanical mode of a specific NEMS.

2.2. GENERAL EQUATIONS FOR THE PULL–IN

In what follows logarithmic derivatives of the energy components will be used. When the dependence of the energy components on the gap is given by a power law, the logarithmic derivatives are simply constants depending on the material properties and the geometry of the NEMS: $\beta_1 = -x\partial \log C/\partial x$, $\alpha_1 = -x\partial \log W/\partial x$, $\beta_2 = x^2 \left(\partial \log C/\partial x\right)^2 + x^2\partial^2 \log C/\partial x^2$ and $\alpha_2 = x^2 \left(\partial \log W/\partial x\right)^2 + x^2\partial^2 \log W/\partial x^2$.

In terms of α and β (which are just numbers by this assumption) the general physical [4] solution satisfying the pull–in conditions (A) and (B) is as follows:

$$\begin{cases} x_o = h\dfrac{\beta_2}{\beta_1+\beta_2}\,\dfrac{1}{2}\left(1+\sqrt{1+4\dfrac{W(x_o)}{kh^2}\,\dfrac{\beta_1+\beta_2}{\beta_2}\,\dfrac{\alpha_2\beta_1-\alpha_1\beta_2}{\beta_2}}\right) \\ \\ V_o = \dfrac{\sqrt{2k}h}{\sqrt{C(x_o)}}\,\dfrac{\sqrt{\beta_2}}{\beta_1+\beta_2}\times \\ \sqrt{\frac{1}{2}-\frac{W(x_o)}{kh^2}\,\frac{(\beta_1+\beta_2)(\alpha_1+\alpha_2)}{\beta_2}+\frac{1}{2}\sqrt{1+4\frac{W(x_o)}{kh^2}\,\frac{\beta_1+\beta_2}{\beta_2}\,\frac{\alpha_2\beta_1-\alpha_1\beta_2}{\beta_2}}}. \end{cases} \tag{2}$$

So far, this expression is still implicit because R.H.S. of the first equation depends on the amount of vdWE at the pull–in gap, $W(x_o)$. However, the vdWE component is normally small at large distances and I propose to substitute the bare value for the pull–in gap $x_o(0) = h\frac{\beta_2}{\beta_1+\beta_2}$ into the R.H.S. of the equations (2). This is allowed for large h because expanding the expression in series in W, one gets the difference of this approximation and an exact result only in the second order of $W/kh^2 \ll 1$. In the opposite limit an explicit solution of the first of Eqs.(2) must be substituted in the second one.

2.3. ROLE OF VAN DER WAALS ENERGY

I present here a specific case of the general equation of state (2) when the electrostatic force can be described via a planar capacitor model: $C = c_o/x$ and the vdW contribution can be written as $W = \varepsilon/h^\alpha$. For completeness, I give here all logarithmic derivative coefficients: $\beta_1 = 1$, $\beta_2 = 2$, $\alpha_1 = \alpha$

[4] Bogus roots of this system of non–linear equations have to be discarded basing on the physical meaning of the solution.

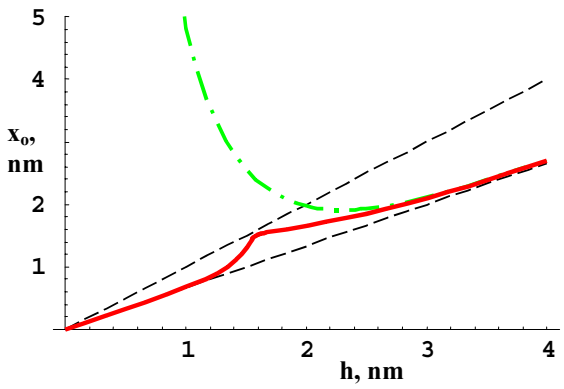

Figure 2. The pull-in gap as a function of the initial device gap. Red (solid) curve represents the selfconsistent result. Green (dash–dotted) curve shows the first–order van der Waals correction. Lower dashed line gives classical MEMS result.

and $\alpha_2 = \alpha(\alpha+1)$. Substituting these values into Eq.(2), I obtain:

$$\begin{cases} x_o = \dfrac{2}{3}h\left(\dfrac{1}{2}+\dfrac{1}{2}\sqrt{1+3\alpha(\alpha-1)\dfrac{W(x_o)}{kh^2}}\right) \\ V_o = \dfrac{2\sqrt{k}h}{3\sqrt{C(x_o)}}\sqrt{\dfrac{1}{2}-\dfrac{3}{2}\alpha(\alpha+2)\dfrac{W(x_o)}{kh^2}+\dfrac{1}{2}\sqrt{1+3\alpha(\alpha-1)\dfrac{W(x_o)}{kh^2}}}. \end{cases} \tag{3}$$

These equations may be further simplified for the small vdW forces: keeping only leading terms in W, I obtain:

$$\begin{cases} x_o \simeq h\dfrac{2}{3}\left(1+\dfrac{3}{4}\alpha(\alpha-1)\dfrac{W(x_o)}{kh^2}+o(W/kh^2)\right) \\ V_o \simeq \dfrac{\sqrt{k}}{\sqrt{c_o}}\left(\dfrac{2}{3}h\right)^{3/2}\left(1-\dfrac{9}{4}\alpha\dfrac{W(x_o)}{kh^2}+o(W/kh^2)\right). \end{cases} \tag{4}$$

The role of the vdW correction is to decrease the pull–in voltage via increasing the pull–in gap: the electrostatic term of the Eq.(1) becomes larger because the vdW force brings the movable electrode closer to the ground plane.

Numerical selfconsistent solutions of the equations (3) are presented in Fig.2 and Fig.3. The classical result (MEMS limit) is shown as a dashed line, a dash–dotted line represents a result of first–order perturbation theory, while solid line represents the selfconsistent solution for the pull–in gap,

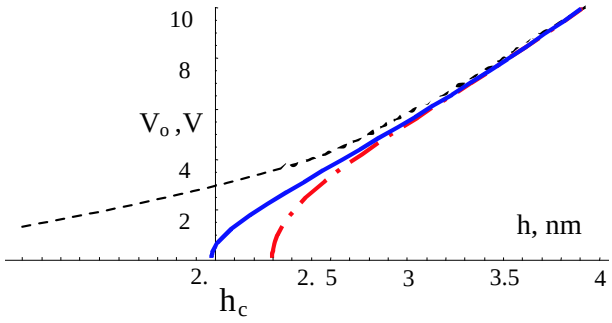

Figure 3. The pull-in voltage as a function of the initial gap. Blue (solid) curve represents the selfconsistent result as explained in the text. Red (dash–dotted) curve shows the dependence in the first–order in van der Waals perturbation. Dashed line shows the classical MEMS result.

x_o, and the pull–in voltage, V_o. The material parameters taken for the numerical estimate are $k = \varepsilon/nm^6$, $c_o = (2/3)\sqrt{k}V/nm$. Typical value for the ε is similar for almost any solid substance and is about several eV Å^6.

In contrast to the classical result, the pull–in voltage as a function of the initial separation, decreases to zero at $h = h_c$ (Fig.3). This is a critical size of a smallest possible nano–electromechanical switch as discussed in Refs. (Dequesnes, 2002a; Rotkin, 2002c).

CONCLUSIONS AND DISCUSSION

In summary, I presented in this section an analytical theory for simulation of an electromechanical system. Using continuum model with a single mechanical degree of freedom, I demonstrated the role of van der Waals forces for nanoscale devices. A general equation of state and a closed form of solution for pull–in parameters are derived for a planar capacitor NEMS. For the NEMS operating at small gaps, the vdW correction is written explicitly. It is discussed how the vdW interaction may restrict applicability of a classical MEMS theory at the distances close to a vdW critical length. This length, derived analytically, gives a principal physical limit for NEMS fabrication. The theory presented in this section allows one to calculate the critical gap as a function of material properties of the nanoswitch (to be found elsewhere).

3. Van der Waals Energy for 1D Systems

In this section I will address theory of the van der Waals interaction in nanotube systems. The van der Waals terms were shown to be extremely important for the NEMS operation in the last section.

The van der Waals interactions have been studied over a considerable period of time. Starting with the phenomenological work of van der Waals (van der Waals, 1873), our understanding has developed from classical models (Reinganum, 1912) to quantum mechanics (London, 1930) and to full statistical quantum electrodynamics (Dzyaloshinskii, 1961). The earlier semi–empirical approach is still considered accurate and adequate for description of many phenomena and it involves transparent physics even for very complex systems.

I model the vdW cohesion[5] following the dielectric function approach. This method was shown to be useful for various solids (Dzyaloshinskii, 1961) and gives a simplest correction within many–body approximation and beyond the 6–12 Lennard–Johns (LJ) potential (Lennard–Jones, 1930).

3.1. CALCULATION OF COLLECTIVE MODES

The theory starts with the calculation of the dielectric function of a single SWNT in RPA neglecting all modes except collective plasmon modes that have most of the oscillator strength. These modes contribute the major input to the total vdWE. For standard semiconductors the dielectric function in a high frequency limit reads as:

$$\varepsilon(\omega) \simeq 1 - \frac{\omega_p^2}{\omega^2}, \tag{5}$$

where ω_p stays for a characteristic plasmon frequency of a material.

Instead of writing the NT dielectric function (refer to papers (Louie, 1995; Li, 2002)) and obtaining its high–frequency limit, I derive the answer from equations of motion of a charge on a cylinder surface:

$$\begin{cases} \dfrac{\partial j}{\partial t} = -\dfrac{ne^2}{m}\nabla\varphi \\ \\ \dfrac{\partial \sigma}{\partial t} + \nabla j = 0 \end{cases}, \tag{6}$$

where $n = 16/3\sqrt{3}b^2$ is the surface electron density in the graphene, m, e are the electron mass and charge, φ is an acting potential on the surface of the SWNT, which includes an induced potential of all charges on the surface, σ is the fluctuation of the charge density related to the plasmon mode, j is its current, ∇ is 2D gradient operator along the surface.

[5] Repulsion is due to the Pauli principle and will not be addressed here.

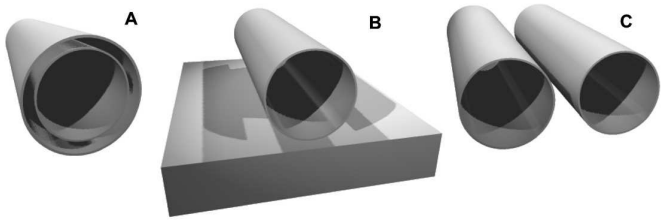

Figure 4. The 1D systems considered in the section. A. Double–shell nanotube. B. Nanotube on a substrate. C. Two nanotubes.

To close the set of equations I write the surface boundary condition for the fluctuation density $\sigma_{k\mu}$ using Gauss–Ostrogradskii theorem:

$$4\pi\sigma_{k\mu} = \varphi_{k\mu}\,\frac{1}{RK_\mu(kR)I_\mu(kR)}, \tag{7}$$

where $K_\mu(kR)$, $I_\mu(kR)$ are Bessel functions of imaginary argument and of order μ taken at the SWNT radius R. k is the co–axial momentum of the mode, μ is the circumferential quantum number of the mode. The plasmon mode frequencies are given by the 1D series for each of allowed $\mu = 0, ..N_{at} - 1$, where N_{at} is the number of atoms along the circumference in one real space unit cell of a SWNT. For example, for [10,10] armchair nanotube it equals 20. The SWNT plasmon dispersion law is:

$$\omega_{k\mu} = \omega_p\sqrt{R^2\left(k^2 + \frac{\mu^2}{R^2}\right)K_\mu(kR)I_\mu(kR)}. \tag{8}$$

Here I use the notation $\omega_p = \sqrt{4\pi ne^2/mR}$ for the 2D plasma frequency, where a characteristic length scale is given by the SWNT radius, R. This frequency sets the energy scale for the collective modes of the tube and, hence, for the vdWE.

3.2. VAN DER WAALS COHESION ENERGY

The vdWE is given by the difference in the total energy of the modes of the electromagnetic vacuum due to the interacting systems approaching each other. The simplest way to calculate it is to find the collective mode frequencies as a function of the distance between the systems. The frequencies depend on the distance because of the Coulomb interaction mixes the modes that are independent for infinite separation. In the zero temperature limit (which is appropriate for distances smaller than 1000 nm), only the zero–point oscillation term survives. The van der Waals force is the derivative of the zero–point oscillation energy with respect to the distance which is implicitly included in the plasmon frequency as it will be shown below.

3.2.1. *Intertube van der Waals attraction*
In this section I calculate the attraction energy between two parallel nanotubes (Fig.4C). I derive the plasmon frequencies from the quantum mechanical Lagrangian within second quantization formalism. The Lagrangian for a single shell is:

$$L_1 = \frac{1}{2}\sum_{k,\mu}\left(\frac{\omega^2}{\omega_{k\mu}^2} - 1\right)\sigma_{k\mu}^{\dagger}\varphi_{k\mu} + h.c., \tag{9}$$

where I use Heisenberg operators of the classical potential, φ, and the classical charge density fluctuation, σ. This form of the continuum Lagrangian is consistent with the equations of motion as given in Eqs. (6). The generalization of the Lagrangian for the case of two tubes (two shells) is straightforward:

$$L = \frac{1}{2}\sum_{k,\mu}\left(\frac{\omega^2}{\omega_{k\mu}^2(1)} - 1\right)\sigma_{k\mu}^{\dagger}(1)\varphi_{k\mu}(1) + \frac{1}{2}\sum_{K,M}\left(\frac{\omega^2}{\omega_{KM}^2(2)} - 1\right)\sigma_{KM}^{\dagger}(2)\varphi_{KM}(2) - \frac{1}{2}\sum_{k,\mu;K,M} V(1-2)\left(\sigma_{k\mu}^{\dagger}(1)\varphi_{KM}(2) + \sigma_{KM}^{\dagger}(2)\varphi_{k\mu}(1)\right) + h.c. \tag{10}$$

where first two terms are the free Lagrangians of the plasmon subsystems and last term represents the interaction between subsystems (1) and (2), which I treat perturbatively. The matrix elements, that represent the Coulomb interaction between the tubes in the continuum limit, are the combinations of the Bessel functions (compare with the exponents in the planar problem (Chaplik, 1971) and the Legendre polynomials in the spherical problem (Rotkin, 1996)). In order to proceed further analytically I restrict the expression for the Coulomb matrix to the components with $k = K$ and $\mu = M$. This approximation has the same accuracy as before because the dimensionless ratio of the interaction to the plasmon energy is small in our problem. One has to keep only the first order of this parameter in the secular equation for the plasmon mixing:

$$\sqrt{\left(-\frac{\omega^2}{\omega_{k\mu}^2(1)} + 1\right)\left(-\frac{\omega^2}{\omega_{k\mu}^2(2)} + \frac{K_\mu(kR_2)I_\mu(kR_2)}{K_\mu(kR_1)I_\mu(kR_1)}\right)} = \mp\frac{I_\mu(kR_2)K_{2\mu}(kD)}{K_\mu(kR_1)} \tag{11}$$

here D is the distance between the tube centers and R_1 and R_2 are the NT radiuses. The shifts of bare plasmon energy levels decrease with k and μ as well as the Coulomb matrix element itself (given by the RHS of Eq.(11)): in the limit of $kD \gg 1$ it approximately equals $1/\sqrt{2\pi\ kD}\exp\ (-k(D-2R))$.

The specific van der Waals energy per atom is the sum of the plasmon zero point oscillation energies divided by the total number of modes. The

integral over the first Brillouin zone of the SWNT has to be substituted for the sum. I have considered the interaction between two tubes of the same radius $\sim$ 7Å. The vdWE derived from the zero–point oscillation of those mixed modes decays with D as $D^{-4.5}$ (presented in Fig.5). In contrast to one–body models this vdWE has a fractional exponent which reflects the specific square root dispersion law of the bare plasmon frequency as given by Eq.(8).

3.2.2. *Cohesion to metal substrate*
The solution obtained for the tube–tube interaction can be readily used to yield the cohesion of the SWNT to the metallic substrate (Fig.4B) because the electric field distribution near a flat conductor is given by an image charge of the opposite sign. Hence, one can choose the odd solution (with the minus sign) of the secular equation (11) while the even solution has to be discarded. The same integration over the Brillouin zone gives now a slower decay of the vdWE. It is because only one subsystem (SWNT) possesses the 1D plasmon modes in this case. The exponent is -3.5 as compared to -4.5 for two SWNTs (Fig.5).

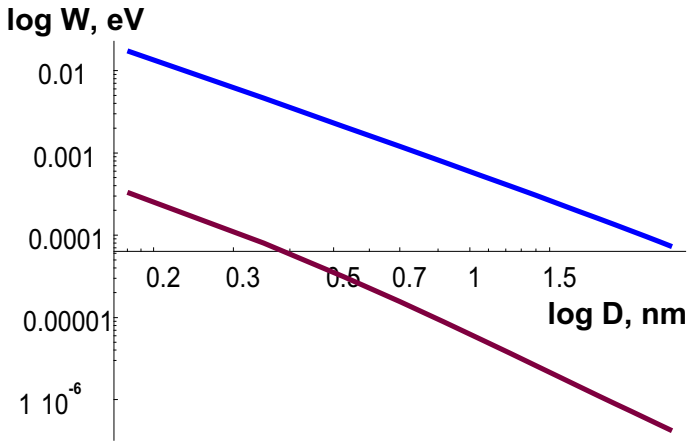

Figure 5. The calculated vdWE: (Upper) for nanotube on a substrate; (Lower) for two identical nanotubes of $R = 7$Å.

3.2.3. *Inter–wall cohesion in DWNT*
The energy of the inter–wall attraction in a multiwall nanotube seemed to be an immeasurable parameter before the discovery of the peapod structures, C_{60}@SWNT, and their transformation in double wall nanotubes (Fig.4A). The process of creation of the second wall inside the initial nanotube is favorable owing to the inter–wall cohesion energy gain.

The Coulomb interaction between shells is given by continuum electrostatics in the same way as before. Because of the axial symmetry of the problem only modes with the same quantum numbers ($\mu = M$, $k = K$) are mixed and the interacting plasmon Lagrangian (10) is exactly diagonal in Fourier space. The secular equation is as follows:

$$\sqrt{\left(-\frac{\omega^2}{\omega_{k\mu}^2(1)}+1\right)\left(-\frac{\omega^2}{\omega_{k\mu}^2(2)}+\frac{K_\mu(kR_2)I_\mu(kR_2)}{K_\mu(kR_1)I_\mu(kR_1)}\right)} = \mp\frac{K_\mu(kR_2)}{K_\mu(kR_1)} \quad (12)$$

The plasmon frequencies depend on the radii of both shells. I plot here the vdW cohesion energy as a function of the intershell distance (Fig.6). This parameter can vary and can be measured experimentally(Iijima, 2001).

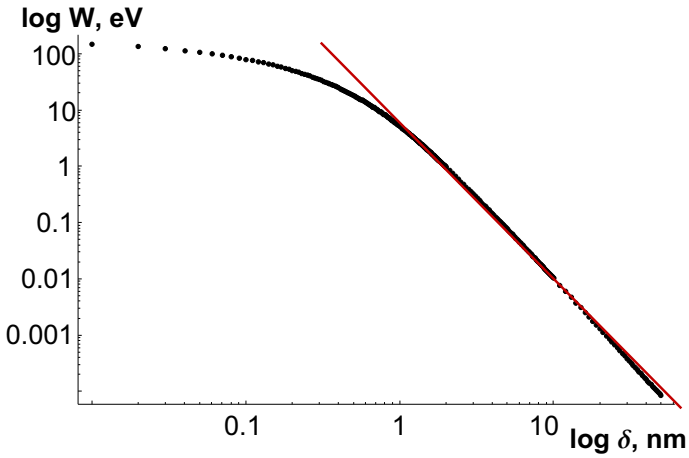

Figure 6. The dependence of the vdWE for a double wall nanotube on the distance between shells, δ (dots); and the linear fit (solid line) with the exponent 2.9.

CONCLUSIONS AND DISCUSSION

In this section a continuum theory has been presented which gives a fast and accurate qualitative estimation of a many–body contribution to dispersion attractive forces for 1D tubular systems made from layered materials. I have used a formalism of a dielectric function and have assumed that main term in the many–body van der Waals cohesion is due to collective modes (plasmons). The plasmon frequencies are explicitly calculated. As a result of the plasmon mixing by the Coulomb interaction, the total system energy is lowered by the van der Waals contribution. A distance dependence of the new (many–body correction) term has a fractional exponent, 5/2 for tube–metal cohesion and 7/2 for tube–tube interaction, unlike an one–body

energy given by LJ 6–12 potential. It was known that a direct summation of the 6–12 atom–atom interactions for the carbon nanotubes gives exponents of 3 and 4 for tube–substrate and intertube cohesion, respectively.

Our approach is almost independent on the structure of interacting lattices, which is in contrast to the one–body LJ potential. It can be easily applied for the cohesion of the tube to not graphitic substrate. This vdWE contribution is especially important for the description of recently studied friction properties of multiwall nanotubes and nanotubes on the graphite (Yu, 2000; Cumings, 2000; Falvo, 2000).

4. Atomistic Electrostatics for Nanotube Devices

Now I switch to how the quantum properties of the nanotubes may reflect in the macroscopic behavior of the nanotube based device. I have already shown in the first section that the capacitance of the nanotube to the backgate is one of important parameters in the modeling of the nanoelectromechanical switch. Recent success in a fabrication of nanotube based nanoelectromechanical devices (Akita, 2001; McEuen, 2002) confirms that this theoretical research is very topical. Here I discuss how the classical meaning of the electrostatic capacitance changes for a nanoscale system. The transport properties of a SWNT device are also determined at some extent by charge distribution along the nanotube channel (Rotkin, 2002d). This charge density can be easily calculated on the base of the theory for the quantum capacitance of the nanotube (Bulashevich, 2002).

4.1. FUNDAMENTALS OF SWNT ELECTROSTATICS

4.1.1. *Classical vs. Quantum Modeling*

The selfconsistent calculation of the equilibrium charge density for the SWNT with a moderate mechanical deformation has been required to support a recent modeling of nanotube electromechanical systems (Dequesnes, 2002a; Dequesnes, 2002b; Rotkin, 2002c). Knowledge of the induced charge allows us calculating an electrostatic energy of the system, which can be rewritten in terms of a distributed capacitance. I demonstrated that this atomistic capacitance has two contributions: purely geometrical term and another one, specific for the nanotube. It is very natural to call the second term "a quantum capacitance" as a similar definition was proposed for a two–dimensional electron gas system in Ref. (Luryi, 1988).

It was found that a statistical description (similar to what was used in Ref.(Odintsov, 2000)) is valid and gives a fairly good estimate for the charge density as compared to the quantum mechanics (see also Sec.4.2.1). The applicability of the macroscopic electrostatics modeling to an equilibrium charge distribution has been already discussed in Refs. (Bulashevich,

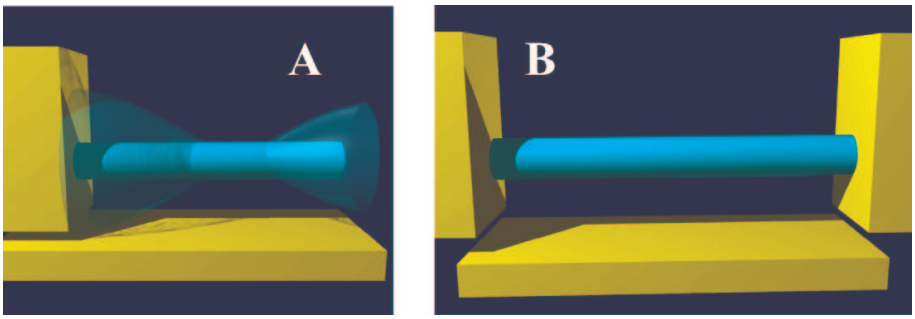

Figure 7. Geometry of two single–wall nanotube devices studied in the section: (A) cantilever NEMS, and (B) string NEMS.

2002; Rotkin, 2002e). Same arguments may hold for a system shifted from equilibrium slightly, *e.g.*, for description of a current carrying device (which can be found elsewhere (Rotkin, 2002d)). The reason for this "classical" behavior of so small quantum object is two–fold. Firstly, the selfconsistent electrostatic energy level shift is the same for every subband of the SWNT in a first approximation (Petrov, 2002). From the other side, the SWNT has a very high depolarization factor as it was noted by Louie (Louie, 1995). The higher the polarization of a molecular system, the closer is the selfconsistent polarizability to its classical limit which is $R^2/2$ for the SWNT (Li, 2002), and R^3 for a spherical fullerene (Rotkin, 1994). The polarization of very mobile pi electrons in nanotubes is very high, hence, one is allowed to apply a "classical" theory, taking into account the quantum mechanical modification of the electronic structure perturbatively.

I studied a SWNT device in a "string" geometry: it comprises the straight nanotube which is fixed (suspended without a slack) between two metal side electrodes over a backgate electrode (Fig.7B). The side electrodes are kept at the same potential with respect to the backgate. This design is standard for electromechanical systems, and the first experimental realization of a single SWNT NEMS appeared recently (McEuen, 2002). I used this and cantilever geometry (Fig.7A) for theoretical study of the nanotube electromechanical switch in Ref.(Dequesnes, 2002a).

4.1.2. *Principles of Compact Model for Nanotube Devices*

The continual compact modeling of the nanotube device bases on three elements: (i) local statistical description of the charge density, (ii) perturbation theory for changes in the charge density due to nanotube deformations and(or) external fields, and (iii) external screening which results in a short range Coulomb potential and allows obtaining analytical expressions. Hypothesis (i) has been proved by comparing the result of the quantum

mechanics with the selfconsistent solution of the Poisson–Boltzmann equations (see Sec.4.2.1). Second supposition is valid until the deformation or(and) axial component of the external field is not too large, which is true for SWNT applications in nanoelectronics but may not fulfill for nano–actuators. The change of the NT density of states with applied external transverse field is studied in Ref. (Li, 2002). It was demonstrated that for the nanotube, which is a one dimensional nanoscale system, it is not possible to separate pure material properties and effects due to geometry/design of the device. The electronic properties of nanotube–in–device differ from what one obtains for a free tube in vacuum.

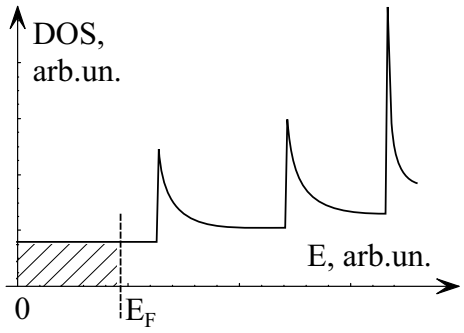

Figure 8. Density of states of a metallic SWNT near the Fermi level: shaded area represents an extra charge induced in the SWNT by shifting the Fermi level away from a charge neutrality level.

4.1.3. *Calculation of Atomistic Capacitance*

In order to calculate the charge distribution of the straight SWNT as a function of the total acting potential I represent the latter as a sum of the external and induced potentials:

$$\varphi^{\rm act} = \varphi^{\rm xt} + \varphi^{\rm ind}. \tag{13}$$

The statistical model supposes that the induced charge is an integral over the nanotube density of states from a local charge neutrality level to a local chemical potential which becomes a Fermi level at zero temperature (see Fig.8). The local chemical potential is supposed to follow the local acting potential. Great simplification is achieved in case of metallic nanotube operating at low voltage when the Fermi level shifts within the first subband. Then, the electron dispersion is linear and the density of states is constant and equals $\nu_M = 8/(3b\gamma)$. Here $b \simeq 1.4$ Å is the interatomic distance and $\gamma \simeq 2.5$ eV is the hopping integral. Within this approximation of the linear energy dispersion in the lowest subband, the induced charge density reads

as:

$$\rho(z) = -e^2 \nu_M \varphi^{\rm act}(z). \tag{14}$$

I note that Eq.(14) holds in one–dimensional (1D) case; while in 2D the charge density is proportional to the electric field (first derivative of the potential) by Gauss–Ostrogradskii theorem, and in 3D the charge density is proportional to the Laplasian of the potential by Poisson equation.

In order to obtain a selfconsistent solution for the charge density I calculate the induced potential with use of a Coulomb operator Green's function, $G(\mathbf{r}, \mathbf{r}')$:

$$\varphi^{\rm ind}(\mathbf{r}) = 4\pi \int G(\mathbf{r}, \mathbf{r}')\rho(\mathbf{r}')\mathbf{dr}'. \tag{15}$$

The Green's function of a 1D system is known to have a logarithmic singularity until some external screening is considered. In case of a nanotube device, this screening is due to the closest gates/contacts. An equation, giving the nanotube charge density implicitly, follows from Eqs.(14,15) and reads as:

$$-\frac{\rho(\mathbf{r})}{e^2\nu_M} - 4\pi \int G(\mathbf{r}, \mathbf{r}')\rho(\mathbf{r}')\mathbf{dr}' = \varphi^{\rm xt}(\mathbf{r}). \tag{16}$$

The equation can be inverted analytically in simple case. In general, it allows only numerical solutions or may be expressed as a series.

An interesting result of our study is that the nanotube may be divided in three parts: two contact regions and a "central" region. The side parts are the regions near the contacts (NT ends) of a length about several h (R) long, where h is the distance to the gate. Aspect ratio of devices of the state–of–the–art of nanotube technology is very high, which means that the length of the nanotube, L, is much larger than the h. Then, the central region of the nanotube covers most of the device length.

The electrostatics of the central region is elementary and allows an analytical solution for Eq.(16). Because of the screening of the Coulomb interaction by the backgate and the valence electrons of the nanotube, the corresponding Green's function is short–ranged. Therefore, (at the distance about $2-3h$ from the contact) the selfconsistent charge density is given by a simple expression:

$$\rho \simeq \rho_\infty = -\frac{\varphi^{\rm xt}}{C_g^{-1} + C_Q^{-1}} \simeq -\varphi^{\rm xt}\, C_g \left(1 - \frac{C_g}{C_Q}\right), \tag{17}$$

here I used notations $C_g^{-1} = 2\log\left(\frac{2h}{R}\right)$ and $C_Q^{-1} = 1/(e^2\nu_M)$ for the inverse capacitance (potential coefficient) of a straight metal cylinder and the quantum correction, respectively. ρ_∞ stands for an equilibrium charge

density of the SWNT, calculated at the distance from the side electrode much larger than the distance to the backgate, h.

4.2. MODEL EXTENSIONS

4.2.1. *Quantum Mechanical calculation*

I derived the Green's functions for several realistic device geometries and calculated the selfconsistent charge densities. These charge densities were compared with the results of the quantum mechanical computation. I solved joint Shroedinger and Poisson equations for the valence pi electrons of a metallic armchair [10,10] SWNT in one subband approximation (in full neglecting the intersubband or sigma–pi mixing which has been estimated and is of minor importance for our problem). Aside such purely quantum effects as quantum beatings at the ends of the finite length nanotube, the statistical, semi–classical and quantum mechanical charge distributions are almost identical (a cross check has been done with use of periodic boundary conditions to exclude the finite length effects). Fig.9A shows the typical charge density distributions calculated with use of a tight–binding theory and the Boltzmann equation for the cantilever SWNT of 50 nm long. I must conclude that a simple statistical description works fairly well for the case of straight ideal single wall nanotube. A similar result has been obtained for the string SWNT with two side contacts (Fig.9B).

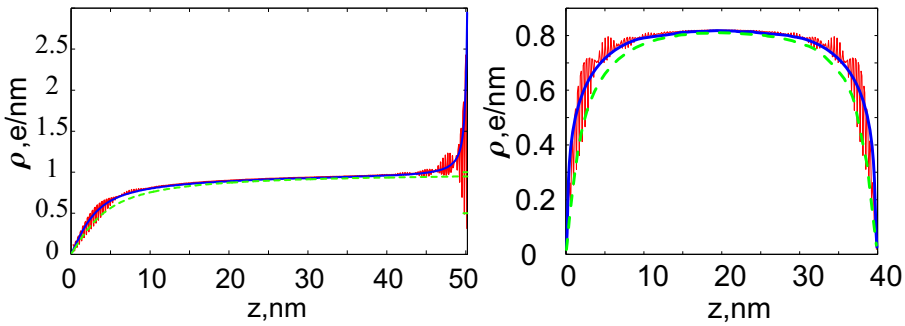

Figure 9. Specific charge density for two devices: (Right) string and (Left) cantilever NEMS. The solid oscillating (red) curve is a result of the quantum mechanical calculation. The solid (blue) line is a solution of joint Poisson and Boltzmann equations. The dashed (green) line is by the analytical approximation.

4.2.2. *Capacitance of Distorted SWNT*

The equation for the equilibrium charge density is valid for a distorted nanotube as well as for an ideal straight nanotube. In case of slightly bent SWNT, one has to use in Eq.(17) the capacitance of the bent metallic

cylinder, $C_g^{-1}(h(z))$, instead of the logarithmic capacitance which is valid only for a straight one. Thus, the atomistic capacitance of the distorted SWNT depends on its shape:

$$C(z) \simeq \frac{1}{C_g^{-1}(h(z)) + C_Q^{-1}} \simeq C_g(z)\left(1 - \frac{C_g(z)}{C_Q}\right). \tag{18}$$

This analytical form of solution for the device electrostatics is very useful for calculating electrostatic forces in various NEMS devices.

CONCLUSIONS AND DISCUSSION

In this section NT electrostatics is studied and equilibrium charge density calculation is performed, which are foundations for a continuum device theory for nanotube electromechanical systems and nanotube electronics. Concept of atomistic capacitance has been introduced. This model gives a fast and accurate method for a simulation of the charge density for the nanotube of an arbitrary shape displaced by a voltage applied to the nanotube end(s). The one–dimensional charge density is given by the total atomistic capacitance of the nanotube, which is not defined solely by material properties of the nanotube itself. It depends also on the environment because of the charge in a low–dimensional electronic system of the nanotube is screened by near placed electrodes. An analytical expression for the atomistic capacitance of a nanotube subjected to moderate distortions is found as well as for an ideal nanotube. The role of quantum effects is evinced and an expression for a NT quantum capacitance is derived.

5. Summary

In this chapter I presented several examples of a state–of–the–art modeling of nanotube device systems and focused on analytical models rather than numerical approaches to give a clear qualitative physical picture of quantum and classical phenomena at the nanoscale. I present the continuum modeling approach which allows one to combine an atomistic computation with a real device engineering, and gives a powerful tool for theoretical study of nanodevices.

Acknowledgements

Author is indebted to Professor K. Hess, Professor N.R. Aluru, and Mr. M. Dequesnes for introducing to the subject of MEMS and fruitful discussions of obtained results, to Dr. A.G. Petrov, Ms. Y. Li and Mr. K.A. Bulashevich for collaboration on the electronic structure computations, and

to Professor Y. Gogotsi, Dr. L. Rotkina and Dr. I. Zharov for fruitful discussions. Author acknowledges support through a CRI grant of UIUC, DoE grant DE-FG02-01ER45932, NSF grant ECS-0210495 and Beckman Fellowship from the Arnold and Mabel Beckman Foundation.

References

S. Akita et. al., Nanotweezers consisting of carbon nanotubes operating in an atomic force microscope, Appl. Phys. Lett. 79(11): 1691–1693, 2001.

N.R. Aluru, J-P. Leburton, W. McMahon, U. Ravaioli, S.V. Rotkin, M. Staedele, T. van der Straaten, B.R. Tuttle and K. Hess, Modeling Electronics on the Nanoscale, *in "Handbook of Nanoscience, Engineering and Technology", Eds.: W. Goddard, D. Brenner, S. Lyshevski, G.J. Iafrate.* CRC Press, 2002.

A. Bachtold, P. Hadley, T. Nakanishi, and C. Dekker, Logic Circuits with Carbon Nanotube Transistors, Science, 294: 1317–1320, 2001.

S. Bandow, M. Takizawa , K. Hirahara, M. Yudasaka, S. Iijima, Raman scattering study of double-wall carbon nanotubes derived from the chains of fullerenes in single-wall carbon nanotubes, Chemical Physics Letters. 337(1-3): 48–54, 2001.

Barash, Iu. S., Sily Van-der-Vaal'sa, Moskva:"Nauka", 1988. 344 p.

L.X. Benedict, S.G. Louie, M.L. Cohen, Static Polarizabilities of Single Wall Carbon Nanotubes, Phys. Rev. B. 52: 8541–8549, 1995.

K.A. Bulashevich, S.V. Rotkin, Nanotube Devices: Microscopic Model, JETP Letters (Transl.: Pis'ma v ZhETF) 75(4): 205–209, 2002.

A.V. Chaplik, Zh.Eksp.Teor.Fiz. (Sov. Phys.–JETP), 60: 1845–1852, 1971.

H. G. Craighead, Nanoelectromechanical Systems, Science, 290: 1532–1535, 2000.

J. Cumings, A. Zettl, Low-Friction Nanoscale Linear Bearing Realized from Multiwall Carbon Nanotubes, Science, 289(5479): 602–604, 28 July 2000.

Dai, H. J., Carbon nanotubes: opportunities and challenges, Surface Science, 500 (1-3): 218–241, 2002.

M. Dequesnes, S. V. Rotkin, and N. R. Aluru, Calculation of pull-in voltages for carbon nanotube-based nanoelectromechanical switches, Nanotechnology, 13: 120–131, 2002.

M. Dequesnes, S. V. Rotkin, and N. R. Aluru, Parameterization of continuum theories for single wall carbon nanotube switches by molecular dynamics simulations, Int.J.Comp.Electronics, 1(3/4): (in press), 2002.

V. Derycke, R. Martel, J. Appenzeller, and P. Avouris, Carbon Nanotube Inter- and Intramolecular Logic Gates, Nano Letters, 1: 453–456, 2001.

Dresselhaus, M. S., Dresselhaus, G., and Eklund, P. C., Science of Fullerenes and Carbon Nanotubes. San Diego, CA: Academic Press, 1996.

I. E. Dzyaloshinskii, E. M. Lifshitz, and L. P. Pitaevskii, Adv. Phys., 10: 165, 1961.

M.R. Falvo, J. Steele, R. M. Taylor II, R. Superfine, Gearlike rolling motion mediated by commensurate contact: Carbon nanotubes on HOPG, Phys Rev. B, 62: 10665–10667, 2000.

L.A. Girifalco, M. Hodak, and R. S. Lee, Carbon nanotubes, buckyballs, ropes, and a universal graphitic potential, Phys.Rev.B-Condensed Matter, 62: 13104–13110, 2000.

P. Kim, C.M. Lieber, Nanotube Nanotweezers, Science. 286: 2148–2150, 1999.

J.E. Lennard–Jones, Perturbation problems in quantum mechanics, Proc. Roy. Soc London, Ser.A, 129: 598–615, 1930.

Y.Li, S.V.Rotkin and U.Ravaioli, Electronic response of nanotubes in transverse electrical field, submitted, 2002.

F. London, Z. Physik, 63: 245, 1930.
S. Luryi, Quantum capacitance devices, Appl. Phys. Lett., 52(6): 501–503, 1988.
E. Minot, V. Sazonova, Y. Yaish, J-Y. Park, M. Brink, P. McEuen, unpublished, 2002.
A.A. Odintsov, Y. Tokura, Journal of Low Temperature Physics, 118: 509, 2000.
P.M. Osterberg, S.D. Senturia, M-test: A test chip for MEMS material property measurement using electrostatically actuated test structures, J. of MEMS, 6(2): 107–118, 1997.
A.G. Petrov, S.V. Rotkin, unpublished, 2002.
M. Reinganum, Ann.d.Phys. Bd., 38: 649, 1912.
V.V. Rotkin, R.A. Suris, Calculation of electronic structure of fullerene within spherical quantum well model, Sov.- Physics of the Solid State, 36 (12): 1899-1905, 1994.
V.V.Rotkin, R.A.Suris, C60 electron collective excitation nature, in *Fullerenes. Recent Advances in the Chemistry and Physics of Fullerenes and Related Materials*. v.III. Eds: R.S.Ruoff and K.M.Kadish. ECS Inc., Pennington, NJ, 1996, 940–959.
S.V. Rotkin, I. Zharov and K. Hess, Zipping of graphene edge results in [10,10] tube formation, *in Electronic Properties of Molecular Nanostructures; (XVth International Winterschool/Euroconference, Kirchberg, Tirol, Austria, 3-10 March 2001), Eds.: H. Kuzmany, J. Fink, M. Mehring, S. Roth. AIP Conference Proceedings*, 591: 454–457, 2001.
S.V. Rotkin, Y. Gogotsi, Analysis of non-planar graphitic structures: from arched edge planes of graphite crystals to nanotubes, Materials Research Innovations. 5(5): 191–200, 2002.
S.V. Rotkin, K. Hess, Many-body terms in van der Waals cohesion energy of nanotubes, Int.J.Comp.Electronics, 1(3/4): (in press), 2002.
S. V. Rotkin, Analytical Calculations For Nanoscale Electromechanical Systems, *in Microfabricated Systems and MEMS – VI, vol. PV 2002–6, Symposium – the Electrochemical Society Proceedings, Eds.: P.J. Hesketh, S.S. Ang, J.L. Davidson, H.G. Hughes, and D. Misra, ECS Inc., Pennington, NJ, USA., 2002*, pp. 90–97.
S.V. Rotkin, A. Shik and H. Ruda, Nanotube and Nanowire Field–Effect Transistors, unpublished, 2002.
S.V. Rotkin, V.Shrivastava, K.A. Bulashevich, and N.R. Aluru, Atomistic Capacitance of a Nanotube Electromechanical Device, *in the Special Issue "Recent Advances in Carbon Nanotubes, Nanoscale Materials and Devices", Eds.: S.V. Rotkin and S. Subramoney.* International Journal of Nanoscience, 1 (6): (in press) 2002.
R. Tenne and A.K. Zettl, Nanotubes from inorganic materials, *in Carbon Nanotubes: Synthesis, Structure, Properties, and Applications, Eds.: Dresselhaus, M. S., Dresselhaus, G., and Avouris, P.; Springer-Verlag, Berlin*, 80: 81-112, 2001.
J.D. van der Waals, Over de Continuepteit van den Gasen Vloeistoftoestand (thesis, Leiden, 1873).
M.F. Yu, B.I. Yakobson, R.S. Ruoff, Controlled sliding and pullout of nested shells in individual multiwalled carbon nanotubes, Journal of Physical Chemistry B, 104: 8764–8767, 2000.